

# Descent isochrones in Martian atmosphere

By Miljan KOLCIC,<sup>1)</sup> Dusan MARCETA<sup>1)</sup>

<sup>1)</sup>Department of Astronomy, Faculty of Mathematics, University of Belgrade, Serbia

(Received February 1st, 2017)

In this paper is presented the analysis of the descent time for ballistic entry, descent and landing (EDL) on Mars and very simple method for optimization of the initial entry parameters, velocity ( $v_0$ ) and flight path angle ( $\gamma_0$ ). Analysis is done using Mars-Gram atmospheric model. The obtained results show that the initial conditions on descent isochrones (lines of constant descent time) have parabolic relationship which enables their optimization by simple solving of the quadratic equation. The specific analysis was performed for EDL of Mars Exploration Rover (MER) for simplified dynamic model, constant aerodynamic parameters and exponential atmosphere, as well as the simulation of EDL in Ptolemaeus Crater in the southern hemisphere for full dynamic, atmospheric and aerodynamic models.

**Key Words:** Mars, atmosphere, trajectory, optimization

## Nomenclature

$\beta$	:	ballistic coefficient
$\gamma$	:	flight path angle
$\lambda$	:	areocentric longitude
$\varphi$	:	areocentric latitude
$\rho$	:	atmospheric density
$\omega$	:	angular velocity of Mars
$A$	:	velocity azimuth
$Cd$	:	drag coefficient
$D$	:	drag force
$g_c$	:	radial component of gravitational acceleration
$g_\varphi$	:	transversal component of gravitational acceleration
$H$	:	scale height
$h$	:	height
$m$	:	mass of the entry vehicle
$r$	:	areocentric radius
$v$	:	velocity relative to the atmosphere
Subscripts		
0	:	initial

## 1. Introduction

The main problem for landing on the surface of Mars is caused by the thickness of its atmosphere, which is approximately hundred of times thinner in atmospheric density than the Earth's. From one side it can cause a significant heating of the entry vehicle, while on the other it can not reduce its terminal velocity to the one necessary for safe landing.

This specifically holds for landing on the southern hemisphere of Mars where the surface elevation is much higher than in the northern lowlands due to Martian dichotomy,<sup>1)</sup> the most prominent feature of its topography. The consequence of this feature is a north-south elevation slope which is shown in Fig. 1

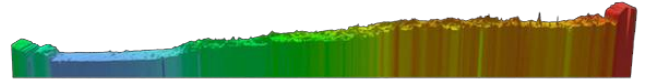


Fig. 1. Mars Orbiter Laser Altimeter (MOLA) pole-to-pole downhill slice along longitude  $0^\circ$ . The south pole is on the right, and the north pole is on the left.<sup>7)</sup>

Since the elevation in the southern highlands is several kilometers higher than in the northern lowlands, landing in these regions requires a special attention to trajectory optimization in order to achieve maximum descent time, which is the key parameter for safe landing because number of complex EDL events has to be performed during this time of the order of tens of seconds. These are the reasons why all successful landings up to date are achieved in relatively low elevations mainly in the northern hemisphere<sup>2)</sup> as it is shown in Fig. 2.

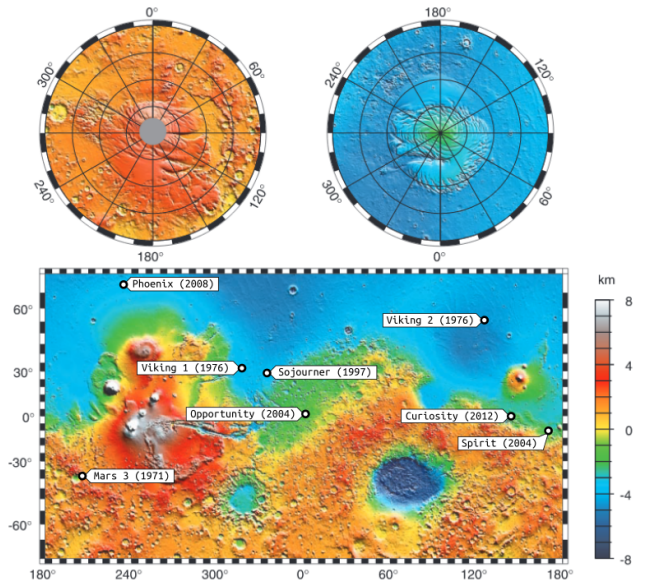


Fig. 2. Maps of Mars global topography from MOLA with landing sites of all successful landings.<sup>6)</sup>

While the landing on the southern hemisphere is extremely difficult from engineering point of view, there is a tremendous

scientific motivation for its exploration, because this part of Martian surface is almost entirely covered with the ancient terrain which originates from the Noachian eon of planetary evolution (4.6 - 3.5 Ga)<sup>3)</sup> and is greatly enhanced by the fact that the majority of locations of confirmed recurring slope lineae (seasonal flows of briny water on today's Martian surface) is in the southern highlands.<sup>4)</sup>

## 2. Trajectory simulation

The only way to control trajectory during the passive ballistic entry is over initial conditions. While one of the main goals in EDL optimization is achieving maximum descent time, it should be borne in mind that the path optimization can not be done by simply determining initial conditions that maximizes this time due to the fact that the initial conditions governs not only the descent time, but also thermal loads, vehicle range whose increase leads to larger deviations from the desired landing location, etc.

Regardless of the problems such as excessive heating and large range, it should be noted that the determination of the maximum descent time as a function of the initial conditions ( $v_0, \gamma_0$ ) does not make much sense, because the velocity at which the vehicle enters the atmosphere is primarily determined by the interplanetary trajectory. For this reason, it could be of a greater importance to determine the dependence of initial conditions which gives a specific descent time, ie. their respective isochrones.

In order to determine in which way initial conditions influences descent time two models are analyzed in this research. The first one is simplified dynamic model with constant aerodynamic characteristics of the vehicle along the trajectory and exponential atmospheric model and the second one is full dynamic model, with realistic aerodynamic models of the vehicle and parachute and realistic atmospheric profile obtained from Mars-GRAM atmospheric model.<sup>5)</sup>

### 2.1. Simplified dynamic, aerodynamic and atmospheric models

For this analysis we used exponential atmospheric model

$$\rho = \rho_0 e^{-\frac{h}{H}} \quad (1)$$

with three different scale heights of 8, 11 and 14 km. The reason for this is very dynamic Martian atmosphere which has extremely large variations of the scale height which is shown in Fig. 3.

Also we used constant ballistic coefficient of  $94 \text{ kg/m}^2$  as it was for MER, and neglected the rotation of the planet. This results in the planar motion of the entry vehicle which can be described with the differential equations of the form:

$$\begin{aligned} \dot{r} &= v \sin \gamma \\ \dot{v} &= -\frac{g}{\beta} - g \sin \gamma \\ \dot{\gamma} &= \cos \gamma \left( \frac{v}{r} - \frac{g}{v} \right) \end{aligned} \quad (2)$$

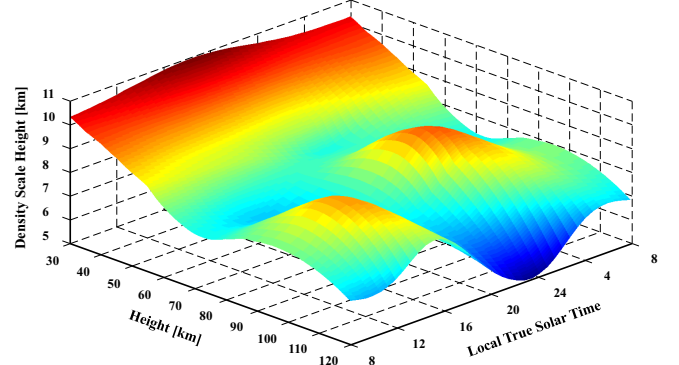


Fig. 3. Diurnal variations of scale height

This analysis was used to determine in which way initial conditions ( $v_0, \gamma_0$ ) affect the descending time from some height defined with the specific value of dynamic pressure. We used the value of 764 Pa as it was for MER entry vehicle.

### 2.2. Full dynamic model

In this part of the analysis we used full dynamic model together with the realistic atmospheric model obtained from Mars-GRAM atmospheric model,<sup>5)</sup> gravity model MRO110,<sup>16)</sup> of degree and order of 110 and also realistic aerodynamic model for the vehicle and for the parachute.

The full entry interface is presented in Fig. 4

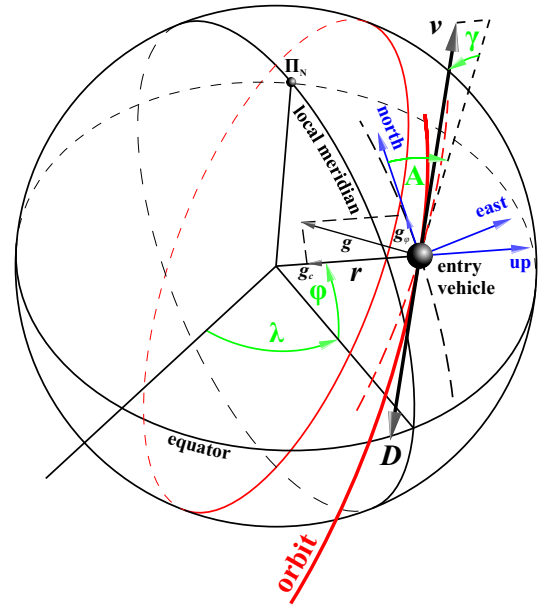


Fig. 4. Entry interface<sup>10)</sup>

To calculate the trajectories of the entry vehicle, a trajectory routine has been developed to integrate 3-degrees-of-freedom trajectory using governing Eq. (3) for translation within the atmosphere, relative to the rotating planet.<sup>8)</sup>

$$\begin{aligned} \dot{r} &= v \sin \gamma, \\ \dot{\varphi} &= \frac{v}{r} \cos \gamma \cos A, \\ \dot{\lambda} &= \frac{v \cos \gamma \sin A}{r \cos \varphi}, \\ \dot{v} &= -\frac{q}{\beta} - g_c \sin \gamma + g_\varphi \cos \gamma \cos A - \\ &\quad \omega^2 r \cos \varphi (\cos \gamma \cos A \sin \varphi - \sin \gamma \cos \varphi), \end{aligned} \quad (3)$$

$$\begin{aligned} v \cos \gamma \dot{A} &= \frac{v^2}{r} \cos^2 \gamma \sin A \tan \varphi \\ &\quad - g_\varphi \sin A + m \omega^2 r \sin A \sin \varphi \cos \varphi \\ &\quad - 2 \omega v (\sin \gamma \cos A \cos \varphi - \cos \gamma \sin \varphi), \\ v \dot{\gamma} &= \frac{v^2}{r} \cos \gamma - g_c \cos \gamma - g_\varphi \sin \gamma \cos A \\ &\quad + \omega^2 r \cos \varphi (\sin \gamma \cos A \sin \varphi + \cos \gamma \cos \varphi) \\ &\quad + 2 \omega v \sin A \cos \varphi. \end{aligned}$$

The trajectory simulation was performed for landing in Ptolemaeus Crater in the southern hemisphere ( $46.2^\circ S$ ,  $202.4^\circ E$ ) with elevation of +1657 m with respect to MOLA reference surface.<sup>9)</sup> This is the site where the only partially successful landing in the southern highlands was achieved by Soviet probe Mars 3 in 1971.

The aerodynamic model, governed by Knudsen and Mach number, which is obtained by the numerical algorithms and experimental procedures for MER, Mars Pathfinder (MPF) and Phoenix (PHX) are presented in Fig. 5.<sup>11)12)13)14)15)</sup>

### 3. Results and Discussion

The main goal of this analysis was to determine in which way initial conditions influence the descent time, which is one of the most important parameters for safe landing. The results obtained by using simplified dynamic and atmospheric model show that descent isochrones, can be approximated very well with parabolas which is shown in figures below.

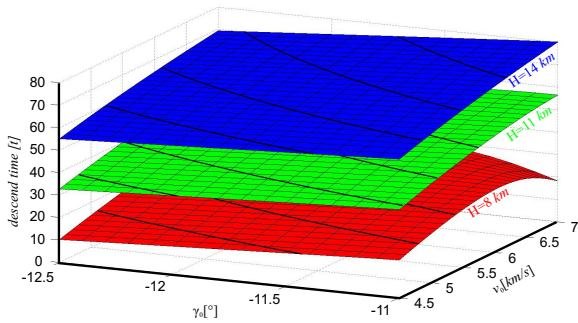


Fig. 6. Descent time for three different scale heights

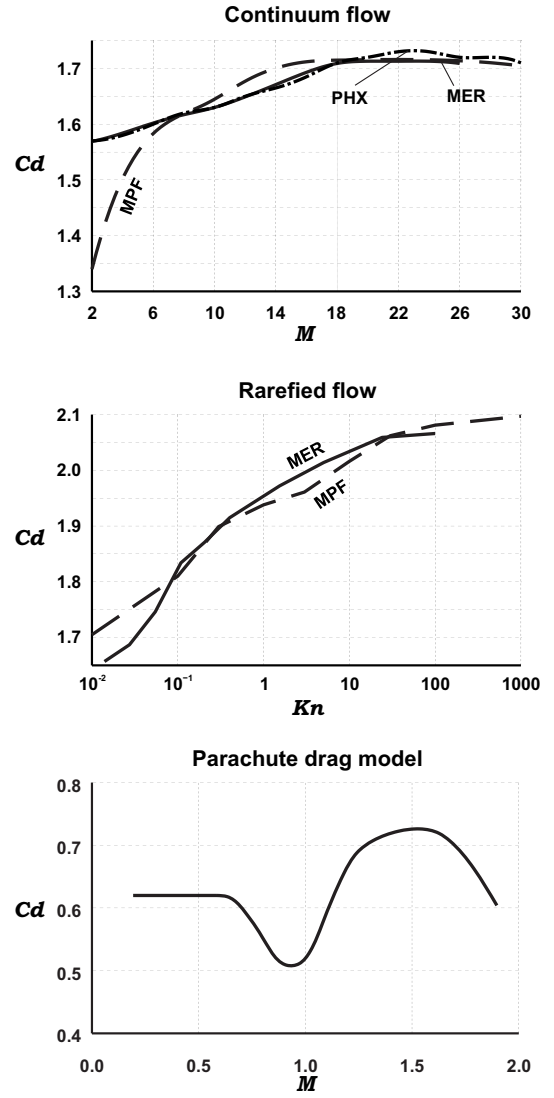


Fig. 5. Aerodynamic model of the entry vehicle and parachute

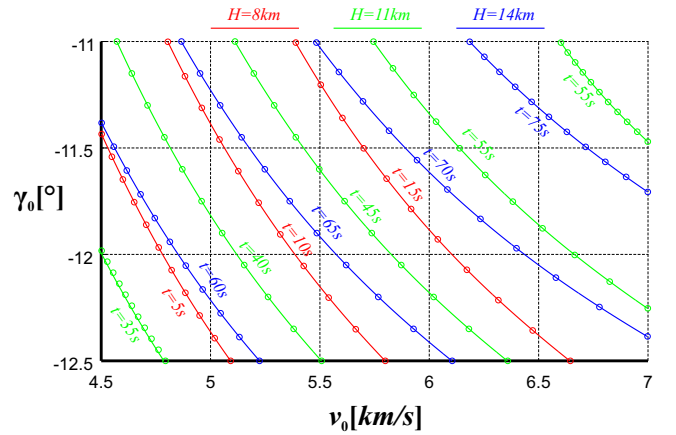


Fig. 7. Descent isochrones and their approximation with parabolas

In Fig. 6 and Fig. 7 one can see that initial conditions ( $\gamma_0$ ,  $v_0$ ) defined by constant descent time from height determined with the dynamic pressure of 764 Pa can be represented with the parabolas. These results indicated the necessity for checking the dependencies of the initial conditions on descent isochrones with full dynamic, atmospheric, gravitational and atmospheric model, because it can allow very simple preliminary optimization of trajectory. In the next two figures are shown the descent

isochrones obtained with full models and their approximation with quadratic curves.

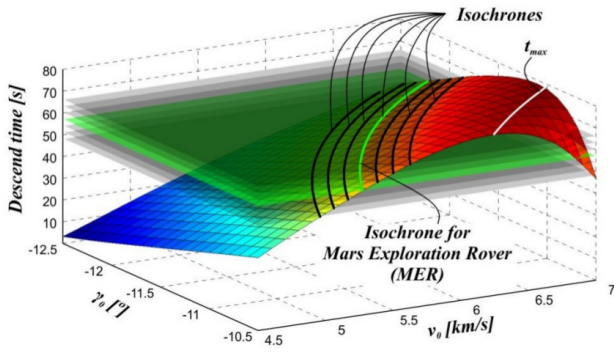


Fig. 8. Descent isochrones for the full models

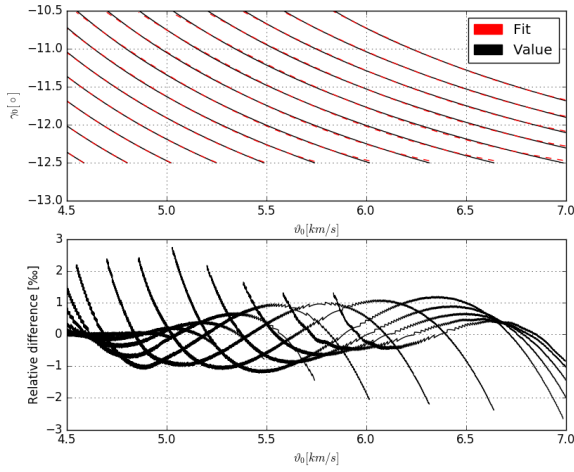


Fig. 9. Descent isochrones and their approximation with parabolas for the full models

In Fig. 8 and 9 one can see that even for full models descent isochrones can be approximated with parabolas very well since the maximum relative error is about 0.2%. Based on these curves, for a certain velocity or the flight path angle, the other parameter that will give the desired descent time could be determined by simple solving of quadratic equation.

The isochrones are fitted with parabolas by using the least squares method which allows to make analytic model for dependence on descent time of initial conditions in the form:

$$\gamma = A(t) \cdot v^2 + B(t) \cdot v + C(t), \quad (4)$$

where coefficients A, B, C are functions of time and also approximated with parabola using least squares method.

$$A(t) = A_1 \cdot t^2 + A_2 \cdot t + A_3 \quad (5)$$

$$B(t) = B_1 \cdot t^2 + B_2 \cdot t + B_3 \quad (6)$$

$$C(t) = C_1 \cdot t^2 + C_2 \cdot t + C_3 \quad (7)$$

In Fig. 10 are shown dependence of coefficients A, B, C on time and in table 1 are given values for their fits Eq. (5) - (7).

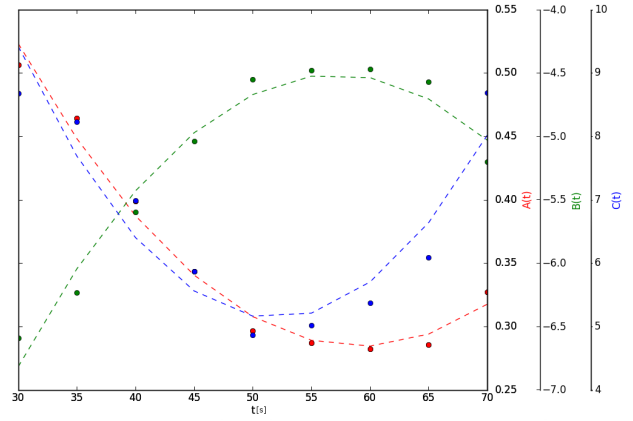


Fig. 10. Dependence of the coefficients on the descent time

Table 1. Coefficients values.

Coefficient	Value
A1	$2.81449767 \cdot 10^{-4}$
A2	$-3.32814538 \cdot 10^{-2}$
A3	1.26813618
B1	$-3.13283396 \cdot 10^{-3}$
B2	$3.57918911 \cdot 10^{-1}$
B3	$-1.47347320 \cdot 10$
C1	$8.88542060 \cdot 10^{-3}$
C2	$-9.23508423 \cdot 10^{-1}$
C3	$2.91239364 \cdot 10$

We analyzed only descent time greater than 30s because 57 seconds was minimal required value for safe landing of MER. In Fig.11 are presented descent isochrones and their approximations, now using the values for the coefficients from the table 1.

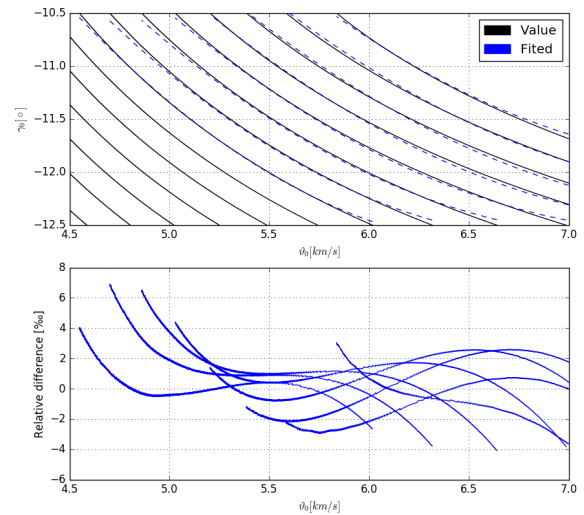


Fig. 11. Comparison of the modeled values with data

We can see that the relative error in determination the corresponding initial flight path angle for a given initial entry velocity is of the order of permille. However, since the trajectory is very sensitive to the initial conditions it is necessary to check how these small deviations affect the descent time. Figure 12 shows two functions of the descent time, one obtained from the

data and the other one with our model and Figure 13 shows their difference.

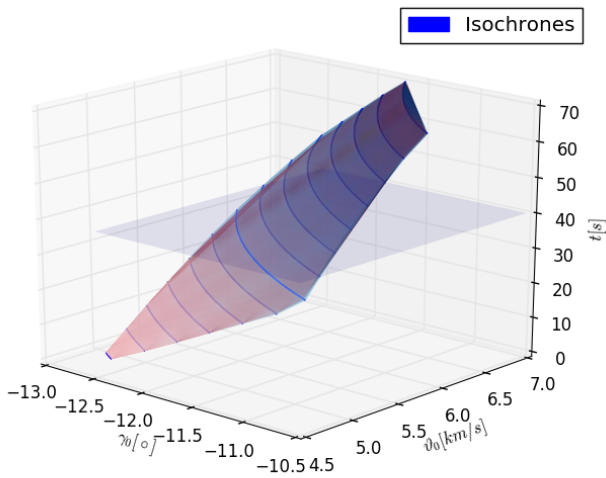


Fig. 12. Descent time depending on the initial conditions

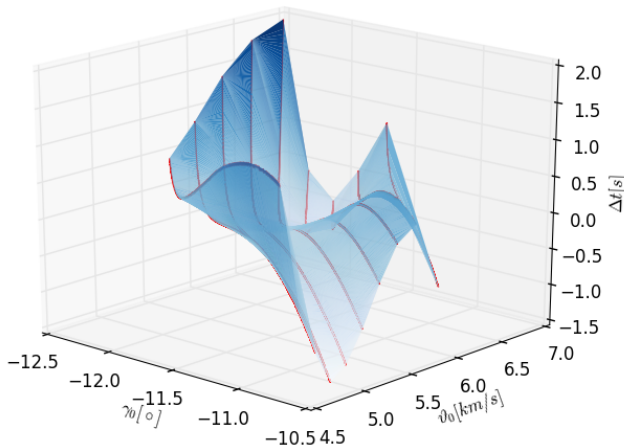


Fig. 13. Deviation in descent times

In these figures one can see that the maximum deviation of the descent time is about 1.5 seconds which appears at the ends of the domains while in the middle of the domains this difference is much lower.

#### 4. Conclusion

From the above analysis several conclusions can be drawn:

- The dependence of the initial conditions on the descent isochrones is parabolic for simplified dynamic, atmospheric and aerodynamic models.
- This dependence for the full models deviates from parabola but the relative difference is very small.

- The developed analytically model gives maximum deviations in the initial conditions of the order of permille. This difference results in the deviation in descent time of maximum 1.5 seconds which is characteristic for the ends of the analyzed domains of  $v_0$  and  $\gamma_0$ .
- Having in mind that the required descent time is of the order of tens of seconds, this model can serve as a very practical tool for preliminary optimization of the EDL trajectory.

#### References

- 1) Smith, D. E. et al.: *The gravity field of Mars: Results from Mars Global Surveyor*, Science, **286** (1999), pp. 94-97.
- 2) Manning, R., and Adler, M.: *Landing on Mars*, AIAA Space 2005 Conference, Long Beach, CA, AIAA Paper 2005-6742, (2005).
- 3) Scott, D. H. et al.: *Geologic Map of Mars*, Misc. Invest. Ser. Map I-1083, U.S. Geol. Surv., Reston, (1978).
- 4) McEwen et al.: *Recurring slope lineae in equatorial regions of Mars*, Nature Geoscience, **7** (2014), pp. 53-58.
- 5) Justus, C. G. et al.: *Mars-GRAM 2000: A Mars atmospheric model for engineering applications*, Advances in Space Research, **29** (2002), pp. 193-202.
- 6) Smith, D. E., Zuber M. T., Solomon S. C., Phillips R. J., Head J. W., Garvin J. B., Banerdt W. B., Muhleman D. O., Pettengill G. H., Neumann G. A., Lemoine F. G., Abshire J. B., Aharonson O., Brown C. D., Hauck S. A., Ivanov A. B., McGovern P. J., Zwally H. J., Duxbury T. C.: *The global topography of Mars and implications for surface evolution*, Science, **284** (1999), pp. 1495-1503.
- 7) Smith, D. E., Zuber, M. T., Frey, H. V., Garvin, J. B., Head, J. W., Muhleman, D. O., Pettengill, G. H., Phillips, R. J., Solomon, S. C., Zwally, H. J., Banerdt, W. B., Duxbury, T. C., Golombek, M. P., Lemoine, F. G., Neumann, G. A., Rowlands, D. D., Aharonson, O., Ford, P. G., Ivanov, A. B., Johnson, C. L., McGovern, P. J., Abshire, J. B., Afzal, R. S., Sun, X.: *Mars Orbiter Laser Altimeter: Experiment summary after the first year of global mapping of Mars*, Journal of geophysical research, **106** (2001), pp. 23689-23722.
- 8) Tewari, A. et al.: *Atmospheric and Space Flight Dynamics: Modeling and Simulation with Matlab and Simulink*, Birkhuser Boston, (2007).
- 9) Smith D.E., Sjogren W.L., Tyler G.L., Balmino G., Lemoine F.G., Konopliv A. S.: *The gravity field of mars: results from mars global surveyor*, Science **286** (1999), pp. 9497.
- 10) Marceta D. et al.: *The effects of the diurnal atmospheric variability on entry, descent and landing on Mars*, **189** (2014), pp. 69-77.
- 11) Gnoffo P. A., Braun R. D., Cruz C. I., Weilmuenster K. J.: *Influence of sonic-line location on mars pathfinder probe aerothermodynamics*, J. Spacecr. Rocket. **33**, **2** (1996), pp. 169177.
- 12) Moss J. N., Blanchard R. C., Wilmoth R. G., Braun R. D.: *Mars Pathfinder Rarefied Aerodynamics: Computations and Measurements*, AIAA paper 98-0298, (1998).
- 13) Schoenenberger M., Cheatwood F.M.: *Static aerodynamics of the mars exploration rover entry capsule*, 43rd AIAA Aerospace Science Meeting and Exhibit, Reno, NV, AIAA paper 2005-0056, (2005).
- 14) Edquist K., Desai P. N., Schoenenberger M.: *Aerodynamics for mars phoenix entry capsule*, J. Spacecr. Rocket. **48**, **5** (2011), pp. 713726.
- 15) Prince J. L., Desai P. N., Queen E. M., Grover M. R.: *Mars phoenix entry, descent, and landing simulation design and modeling analysis*, J. Spacecr. Rocket. **48**, **5** (2011), pp. 756764.
- 16) Konopliv A. S., Asmar S. W., Folkner, W. M., Karatekin Ö., Nunes D. C., Smrekar S. E., Yoder C. F., Zuber M.T.: *Mars high resolution gravity fields from MRO, Mars seasonal gravity, and other dynamical parameters*, Icarus, **211** (2011), pp. 401-428.